

logarithmic derivative of phonon frequency with respect to uniform strain, that is, $\gamma = (\partial \ln \nu / \partial \ln V)_k$.

For a variety of liquids, the pressure-dependence of $(\Delta T / \Delta P)_S$ at high pressure is small. The calculation of γ in Table 1 is therefore extended by extrapolation to 2.9 GPa of results up to 2.4 GPa. As for the other liquids where the isothermal pressure-dependence of γ is known [Hg, water, pentane, and isopentane (10)], in contrast to solids (11) and Earth's mantle and core (12), the Grüneisen parameters of ethanol and methanol increase with decreasing volume.

It is the evaluation of the second term on the right side of Eq. 2, the "correction" of the experimentally determined adiabatic compressibility to the isothermal compliance $[K_S^{-1} = K_T^{-1} - \alpha(\partial T / \partial P)_S]$, that constitutes the principal source of uncertainty in this preliminary study. The direct measurement of $(\Delta T / \Delta P)_S$ by Boehler and Kennedy (10) and the classical study of the P - V - T relations of methanol by Bridgman (6) do, however, serve to determine this correction over the range of pressure wherein it is large (Fig. 4) and provide a basis for the deduction of the pressure-volume relations at higher pressures. The experimental pressure-dependence of the correction and the smooth curve used in the integration of Eq. 2 are given in Fig. 4.

The correction term in Eq. 2 can also be expressed as $\alpha^2 T / C_p$. The pressure dependence of this quantity is implicit in the P - V - T relations and so may be approximated recursively from sound velocity data at a series of temperatures (13). Thus, laser-induced phonon spectroscopy in the diamond-anvil cell offers an approach to the determination of acoustic velocities and the

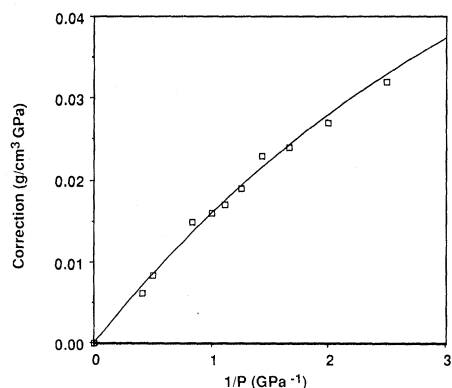


Fig. 4. The second term in Eq. 2 (that is, the density times the difference between the isothermal and adiabatic compressibilities) calculated from $(\Delta T / \Delta P)_S$ (10) and the coefficient of thermal expansion (6), plotted with open squares, and extrapolated (solid curve) to higher pressures. The estimated uncertainty in the correction is comparable with the scatter of the experimental points.

equation of state at high compression. In these preliminary studies we have sought to compare the results obtained at the lower end of the range conveniently investigated in the diamond-anvil cell with those obtained by other techniques and to extend the equation of state of methanol to higher compressions than have been investigated by the conventional piston-cylinder techniques. The technique reported here should be quite generally applicable. We have, for example, observed strong scattering from thermally excited quasilongitudinal and quasitransverse waves in olivine at high pressure (5). As another example, less than 0.5% water produces a useful signal from N_2 in the diamond-anvil cell.

REFERENCES AND NOTES

1. Y. X. Yan, L. T. Cheng, K. A. Nelson, in *Advances in Non-linear Spectroscopy*, J. H. Clark and R. E. Hester, Eds. (Wiley, London, 1987), pp. 299-354.
2. M. D. Fayer, *Annu. Rev. Phys. Chem.* **33**, 63 (1982).
3. K. A. Nelson, R. J. D. Miller, D. R. Lutz, M. D. Fayer, *J. Appl. Phys.* **53**, 1144 (1982).
4. H. K. Mao and P. M. Bell, *ibid.* **49**, 3276 (1978).
5. J. M. Brown, L. J. Slutsky, K. A. Nelson, L.-T. Cheng, in preparation.
6. P. W. Bridgman, *Proc. Am. Acad. Arts Sci.* **74**, 403 (1942); *International Critical Tables* (McGraw-Hill, New York, 1928), vol. 3, p. 41.
7. We initiate the integration at 1.96 GPa because (i) Bridgman's data are quite accurate at and below this pressure range and (ii) integration with sparse data at the lowest pressures (where velocities increase rapidly with pressure) tended to be unstable.
8. G. J. Piermarini, S. Block, J. D. Barnett, *J. Appl. Phys.* **44**, 5377 (1973).
9. W. Wilson and D. Bradley, *J. Acoust. Soc. Am.* **36**, 333 (1964).
10. R. Boehler and G. C. Kennedy, *J. Appl. Phys.* **48**, 4183 (1977).
11. R. Boehler and J. Ramakrishnan, *J. Geophys. Res.* **85**, 6696 (1980).
12. J. M. Brown and T. J. Shankland, *Geophys. J. R. Astron. Soc.* **66**, 579 (1981).
13. R. L. Mills, D. H. Liebenberg, J. C. Bronson, *J. Chem. Phys.* **63**, 1198 (1975).
14. This work was supported by NSF grants DMR-8704352 (K.A.N. and L.-T.C.) and EAR-8618573 (J.M.B. and L.J.S.).

22 March 1988; accepted 24 May 1988

Brownian Dynamics of Cytochrome c and Cytochrome c Peroxidase Association

SCOTT H. NORTHRUP,* JEFFREY O. BOLES, JOHN C. L. REYNOLDS

Brownian dynamics computer simulations of the diffusional association of electron transport proteins cytochrome c (cyt c) and cytochrome c peroxidase (cyt c per) were performed. A highly detailed and realistic model of the protein structures and their electrostatic interactions was used that was based on an atomic-level spatial description. Several structural features played a role in enhancing and optimizing the electron transfer efficiency of this reaction. Favorable electrostatic interactions facilitated long-lived nonspecific encounters between the proteins that allowed the severe orientational criteria for reaction to be overcome by rotational diffusion during encounters. Thus a "reduction-in-dimensionality" effect operated. The proteins achieved plausible electron transfer orientations in a multitude of electrostatically stable encounter complexes, rather than in a single dominant complex.

BIOLICAL PROCESSES ON A MOLECULAR level require the transport of reactants through space by a diffusional mechanism leading to a reactive event (1). In many cases the diffusional encounter of species limits the overall rate, and thus a knowledge of the dynamics of such encounters is of fundamental importance in the understanding of the biological event. Usually, one or more of the species is a macromolecule having a small reactive region relative to its overall size, which can lead to very severe orientational criteria for reaction. Adam and Delbruck (2) proposed that in order to overcome the formidable obstacle posed by the required translational and rotational search process, the efficiency of biochemical systems may be optimized by exploiting the so-called reduction-in-dimensionality principle, in which the molecular

species diffuse in a three-dimensional space and initially associate in unreactive configurations by ubiquitous nonspecific forces of attraction, either of a Coulombic or van der Waals type. This association is followed by a diffusional search on a lower dimensional configurational surface of associated particles that increases the probability of ultimate production of a properly oriented pair. The magnitude of forces promoting the initial nonspecific association must be finely tuned to a range allowing particles to remain in juxtaposition for time scales required for the lower dimensional diffusive search, but not so strong that encountered particles are locked into unproductive orientations. This

Department of Chemistry, Tennessee Technological University, Cookeville, TN 38505.

*To whom correspondence should be addressed.

Table 1. Frequencies of the most frequent occurrences of triads of ionic contacts in docked complexes of cyt c and cyt c per.

Cyt c per residue	Cyt c residue	Frequency
Asp ³⁴ /Glu ³⁵ Glu ²⁰⁹ Glu ²⁹⁰	Lys ⁷⁹ Lys ¹³ Lys ²⁵ /Lys ²⁷	11
Asp ³⁴ /Glu ³⁵ Glu ¹⁸⁸ Asp ²¹⁷	Lys ¹³ Lys ²⁵ /Lys ²⁷ Lys ²⁵ /Lys ²⁷	8
Glu ²⁰¹ Glu ²⁰⁹ Glu ²⁹⁰	Lys ⁷⁹ Lys ⁷⁹ Lys ⁷²	8
Asp ³⁴ /Glu ³⁵ Glu ²⁰¹ Glu ²⁰⁹	Lys ¹³ Lys ⁷⁹ Lys ⁷⁹	7
Asp ³⁴ /Glu ³⁵ Glu ²⁰¹ Glu ²⁹⁰	Lys ⁷⁹ Lys ²⁵ /Lys ²⁷ Lys ²⁵ /Lys ²⁷	7
Asp ³⁴ /Glu ³⁵ Glu ²⁰¹ Glu ²⁹⁰	Lys ¹³ Lys ⁷⁹ Lys ⁷²	6
Asp ³⁴ /Glu ³⁵ Asp ³⁴ /Glu ³⁵ Glu ²⁰¹	Lys ¹³ Lys ⁸⁶ Lys ⁷⁹	6

at random heme-plane orientation is twice the experimental value. A tenfold retardation of the rate was observed in the absence of electrostatic forces for reasonable choices of geometric reaction criteria at ionic strength $I = 0.1m$. For the same geometric case as above, for instance, the diffusional association rate constant is $0.41 \times 10^8 M^{-1} s^{-1}$ in the absence of forces. This result is not surprising, in that cyt c and cyt c per possess large, oppositely charged monopoles (+8e and -12e, respectively) at pH 7. Furthermore, cyt c has a preponderance of positive charges around its heme edge, whereas cyt c per has negatively charged residues at its heme exposure regions. Rate constants were computed at three ionic strengths, and ionic strength behavior corresponded closely with that observed experimentally in the physiological regime, as has been previously discussed (7).

Cyt c and cyt c per are able to successfully achieve realistic geometric criteria for electron transfer ($d_{edge} < 20 \text{ \AA}$ and $\Psi < 30^\circ$) from a large ensemble of encounter complexes that are virtually all electrostatically stable, rather than from a single dominant protein-protein complex. This multitude of potentially productive electron transfer complexes form three distinct and widely separated domains on cyt c per (Fig. 1). These regions are in a belt approximately in the cyt c per heme plane and coincide with the electrostatically attractive regions observed in that plane (Fig. 2). The most predominant of these regions matches the region around Asp³⁴ of cyt c per hypothesized by Poulos and Kraut (17) in their

model-building of a plausible electron transfer complex. The second region is substantially removed from the first region and is centered around Asp¹⁴⁸. A third, less populated region intermediate between these two dominant areas is the area near Asp²¹⁷ on cyt c per. The existence of a large, nonspecific ensemble of stable encounter complexes is reminiscent of the observed behavior in the similar case of cyt c and cytochrome b₅ docking (18).

An analysis of the electrostatic contacts giving rise to stability of the multitude of encountered states was performed. The triads of electrostatic contacts that occur most frequently in 243 complexes with favorable geometric criteria for electron transfer are listed in Table 1. This frequency distribution implies a nonspecific Coulombic binding process, in which a predominantly positive surface of cyt c interacts with several predominantly negative surfaces of cyt c per. At any given time, there appear to be three or four interprotein ionic contacts that stabilize the encounter complexes.

Figure 2 is an interprotein potential energy contour map around cyt c per in its heme plane as a function of the center of mass of the incoming cyt c. At each relative position of the centers of mass of the two proteins, we performed a Boltzmann average of the potential energy over all accessible rotational orientations of the incoming cyt c protein by Monte Carlo sampling. Note the existence of an extensive electrostatic channel of a depth of between 1 to 2 units of $k_B T$ (where k_B is Boltzmann's constant and T is the temperature) that spans the three docking regions. This channel provides a lower dimensional region by which the incoming translating and rotating cyt c may engage in an extended exploration of the surface of cyt c per in search of a productive electron transfer configuration. From analysis of dynamics of trajectories, we found that in a typical encounter of these two proteins, the encounter is quite prolonged (10² ns), and cyt c undergoes numerous rotational reorientations (rotational relaxation time ~ 6 ns) as it explores an extensive region on the surface of cyt c per, and may even include all three major docking regions in one excursion. A single typical encounter trajectory is depicted in Fig. 3, in which the field of blue, red, and green dots represents the positions at various instants of time of a point on the front surface of cyt c as it diffuses around the larger cyt c per molecule shown in magenta. The color of the dots indicates the rotational state of cyt c as described in the caption, blue meaning that the cyt c-exposed heme edge is oriented toward cyt c per, green meaning it is facing away, and red being an intermediate orientation. The orientation of

cyt c changes numerous times during this single encounter. The bands of red and green are at about one and two cyt c radii from the cyt c per surface, respectively, meaning that the two proteins are still in contact but in an unfavorable orientation for reaction. The proteins thus explored a wide variety of mutual orientations in a single encounter.

Additional simulations in which lysines were selectively mutated into -1e charges on the heme-edge side and the side opposite the heme edge of cyt c were performed to observe any changes in the rate constant at physiological ionic strength (8). Interestingly, the charge-reversal mutations of Lys²² and Lys³⁹, which both occur on the backside of cyt c, had little effect (1% and 11% increase, respectively) on the rate constant, despite the accompanying perturbation of the dipole moment of cyt c.

With the rigid protein geometries used here, the closest heme-edge distance attained was 18 Å, and that only rarely, whereas model studies (17) have constructed complexes with distances of 16.5 Å by allowing side chains to reorient. This result is consistent with the molecular dynamics study (19) of a particular docked complex of cyt c and cytochrome b₅ of Wendoloski *et al.*, in which protein dynamics allowed a contraction of the heme-heme distance by several angstroms on a picosecond time scale.

Several design principles of these cytochromes emerge that are deemed to be essential in order to account for the results presented here. First, the tenfold rate enhancement upon electrostatic-force inclusion confirms the hypothesis (20) that the electrostatic forces strongly enhance the encounter of these proteins in favorable geometries for reaction. Second, the existence of two and possibly three distinct, separated domains on cyt c per in a belt approximately in the cyt c per heme plane coinciding with the electrostatically attractive regions shows a strong relation between electrostatic details and electron transfer geometry restrictions in the design of these proteins. A unique, dominant stable reactive complex was not found. Furthermore, the results lend additional support to the hypothesis of two distinct binding areas on cyt c per for cyt c rather than one (21). Third, our study provides evidence that at least partial heme-plane alignment is necessary for electron transfer to occur. Since inclusion of side-chain reorientation to optimize electrostatic binding is likely to increase the simulated rate under all of the geometric cases considered, the implication is that the electron transfer mechanism will involve at least partial alignment of the heme planes, probably

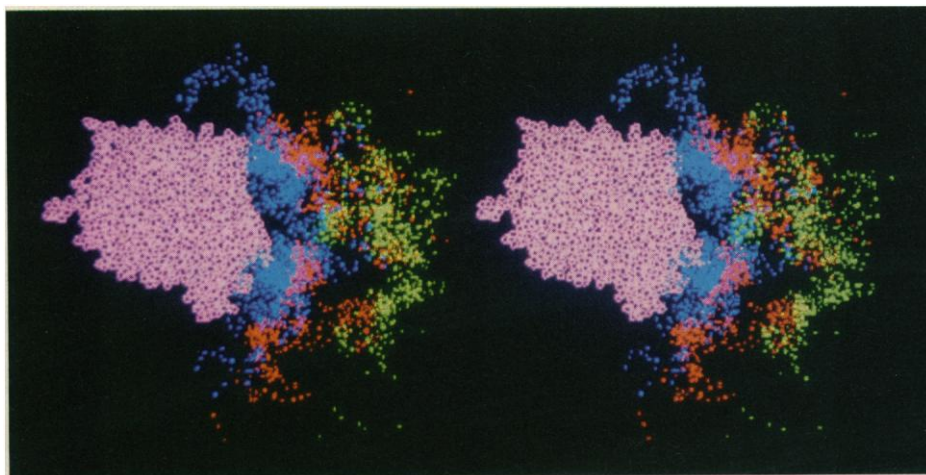


Fig. 3. Stereoscopic projection depicting the computer-simulated history of a single typical diffusive encounter between cyt c and cyt c per leading to electron transfer. A space-filling model of the larger cyt c per protein is shown in magenta, in basically the same orientation as Figs. 1 and 2. The surrounding field of blue, red, and green dots represents the time evolution of a point on the heme edge face of cyt c. The color scheme of the dots represents the rotational state of the diffusing cyt c protein. The rotational state is determined by a heme director vector (a vector from center of mass of cyt c to the point on the front heme surface). Blue, red, and green indicate that the heme director vector makes an angle that is within the interval (0° , 30°), (30° , 60°), and (60° , 90°) of the vector between protein centers, respectively.

with a value of Ψ smaller than the 60° we have predicted here. This study also confirms the hypothesis that this reaction is diffusion-controlled (20). Association rate constants simulated here are at the upper limit, in which electron transfer is instantaneous upon achieving very liberal geometric criteria, and are still in agreement with actual experimental rate constants for electron transfer (16). Fourth, the widely distributed frequency of ionic contacts (with three or four interprotein salt bridges stabilizing encounter complexes) shows that there is a not strict charge complementarity in operation that locks the proteins into a single electron transfer arrangement, but that association is more nonspecific in nature. The charge perturbation study provides additional evidence that global dipole-dipole and monopole-dipole interactions between these proteins are of little consequence relative to the local ionic contacts between the heme-edge regions. Fifth, the electrostatic forces provide the appropriate range of attractive potential energy to allow a reduction-in-dimensionality effect to operate. The protein thus can explore a wide variety of mutual orientations in a single encounter, rather than being deterministically steered by Coulomb forces over long distances into one selective docking arrangement, depositing the electron, and then diffusing apart. Finally, surface side chain flexibility must play an important role (22) in facilitating the docking and overall stability of encountered proteins, and further enhance electron transfer by allowing the heme groups to attain much closer positions than simulated here.

Brownian dynamics study provides an important complement and interface to other computational approaches reported recently in the literature. Sharp *et al.* (4) presented results of Brownian simulations of a small ion diffusing in the electrostatic field generated by the protein superoxide dismutase. Our more computationally demanding protein-protein association study is an important extension of Brownian dynamics into an exciting and important new area of more complex substrates. Our simulations are specifically designed to explore the initial diffusional approach and casual association of two proteins on time scales of nanoseconds in which each Brownian step represents tens of picoseconds. The numerous complexes we have generated should provide appropriate starting structures for subsequent molecular dynamics simulations of docked complexes such as reported recently by Wendoloski *et al.* (19). Their simulations of motion of the cyt c-cytochrome b_5 electron transfer complex provide a description of how protein internal flexibility allows a more intimate complex to be formed on time scales of a few picoseconds for facilitating electron transfer. Molecular dynamics simulation has the added advantage of explicit incorporation of water molecules that may interpose themselves at the complex interface. A complement to both of these studies is the computation of actual electron tunneling pathways in cytochrome proteins by the method of Kuki and Wolynes (23). A combination of these interfacing computational methodologies thus has the potential of answering many of the questions that remain concerning the geometrical and

physical requirements for control of electron transfer in biological organisms, particularly since information about transient complexes cannot be gained easily by present structural methods.

Brownian dynamics simulations with a more refined reaction criterion for electron transfer and with some inclusion of protein flexibility has the potential for predicting the wide range of reactivity differences observed in the cytochromes, and is not limited to diffusion-controlled cases. In the rapid diffusion limit, the BD algorithm provides an efficient way of generating the equilibrium distributions of electron transfer complexes necessary for calculating rate constants controlled by electron transfer.

REFERENCES AND NOTES

- O. G. Berg and P. H. von Hippel, *Annu. Rev. Biophys. Biophys. Chem.* **14**, 131 (1985).
- G. Adam and M. Delbruck, in *Structural Chemistry and Molecular Biology*, A. Rich and N. Davidson, Eds. (Freeman, San Francisco, 1968), pp. 198-215.
- J. B. Matthew and D. H. Ohlendorf, *J. Biol. Chem.* **260**, 5860 (1985).
- K. Sharp *et al.*, *Science* **236**, 1460 (1987).
- K. Sharp, R. Fine, K. Schulten, B. Honig, *J. Phys. Chem.* **91**, 3624 (1987).
- S. A. Allison *et al.*, *ACS Symp. Ser.* **302**, 216 (1986); S. A. Allison, G. Ganti, J. A. McCammon, *Biopolymers* **24**, 1323 (1985); S. A. Allison and J. A. McCammon, *J. Phys. Chem.* **89**, 1072 (1985).
- S. H. Northrup *et al.*, *J. Phys. Chem.* **91**, 5991 (1987).
- S. H. Northrup, J. A. Luton, J. O. Boles, J. C. L. Reynolds, *J. Comput. Aided Mol. Design*, in press.
- S. H. Northrup, S. A. Allison, J. A. McCammon, *J. Chem. Phys.* **80**, 1517 (1984); S. A. Allison, S. H. Northrup, J. A. McCammon, *ibid.* **83**, 2894 (1985); S. H. Northrup, M. Curvin, S. A. Allison, J. A. McCammon, *ibid.* **84**, 2196 (1986); S. H. Northrup, J. D. Smith, J. O. Boles, J. C. L. Reynolds, *ibid.*, p. 5536; G. Ganti, J. A. McCammon, S. A. Allison, *J. Phys. Chem.* **89**, 3899 (1985).
- T. Takano and R. E. Dickerson, *Proc. Natl. Acad. Sci. U.S.A.* **77**, 6371 (1980).
- B. C. Finzel, T. L. Poulos, J. Kraut, *J. Biol. Chem.* **259**, 13027 (1984).
- F. C. Bernstein *et al.*, *J. Mol. Biol.* **112**, 535 (1977).
- S. H. Northrup *et al.*, *J. Am. Chem. Soc.* **108**, 8162 (1986).
- J. Warwicker and H. C. Watson, *J. Mol. Biol.* **157**, 671 (1982).
- I. Klapper, R. Hagstrom, R. Fine, K. Sharp, B. Honig, *Protein Struct. Funct. Genet.* **1**, 47 (1986).
- C. H. Kang, D. L. Brautigan, N. Osheroff, E. Margoliash, *J. Biol. Chem.* **253**, 6502 (1978).
- T. L. Poulos and J. Kraut, *ibid.* **255**, 10322 (1980).
- M. R. Mauk *et al.*, *Biochemistry* **25**, 7085 (1986).
- J. J. Wendoloski *et al.*, *Science* **238**, 794 (1987).
- E. Margoliash and H. R. Bosshard, *Trends Biochem. Sci.* **8**, 316 (1983).
- C. H. Kang *et al.*, *J. Biol. Chem.* **252**, 919 (1977); J. A. Kornblatt and A. M. English, *Eur. J. Biochem.* **155**, 505 (1986); L. B. Vitello and J. E. Erman, *Arch. Biochem. Biophys.* **258**, 621 (1987).
- J. B. Matthew and J. J. Wendoloski, *Biophys. J.* **51**, 404a (1987).
- A. Kuki and P. G. Wolynes, *Science* **236**, 1647 (1987).
- This work has been made possible by grants DK01403 and GM34248 from the National Institutes of Health and by grant 17051-B7 from the Petroleum Research Fund as administered by the American Chemical Society. S.H.N. is the recipient of an NIH Research Career Development Award.

2 February 1988; accepted 4 May 1988